PROCEEDINGS OF SCIENCE

# ANTARES search for point sources of neutrinos with 11 yr of data: a likelihood stacking analysis

**The ANTARES[‡] Collaboration**
[‡] *http://antares.in2p3.fr/Collaboration/index2.html*
*E-mail:* julien.aublin@apc.in2p3.fr

A search for astrophysical neutrino sources using the data collected by the ANTARES detector between January 29, 2007 and December 31, 2017 is presented. A likelihood stacking method is used, allowing the significance of a global excess of neutrino events in correlation with catalogs to be assessed.
Different catalogs are considered: a) a sub-sample of the Fermi 3LAC, b) a star-forming galaxy catalog, c) a sample of giant radio-galaxies, and d) a jet-obscured AGN population.
The star-forming galaxies in b) were selected in the GeV range by Fermi-LAT, and have been used in a recent analysis by the Pierre Auger Collaboration. The catalog c) is built from radio and soft gamma-ray surveys (SWIFT-BAT and INTEGRAL), and it contains the brightest and most accretion-efficient radio galaxies with a double lobed radio morphology. The catalog d) provides a complementary test with the jet-obscured AGN morphology, where an enhanced neutrino production is expected, whereas UHECRs and gamma-ray production are damped.
As an additional and independant test, the correlation of ANTARES neutrinos with 51 public track events from IceCube is evaluated: 36 tracks from the 8 year up-going muons (deposited energy above 200 TeV) and 15 additional tracks from the 6 year HESE sample are used for this study.

*36th International Cosmic Ray Conference -ICRC2019-*
*July 24th - August 1st, 2019*
*Madison, WI, U.S.A.*

 

PoS(ICRC2019)840

## 1. Introduction

The ANTARES neutrino telescope, a water Cherenkov detector operating since 2007 under the Mediterranean Sea 40-km off-shore Toulon, is detecting high energy neutrinos by observing the passage in water of relativistic particles produced by interactions of neutrinos in the vicinity of the instrumented volume. Neutrinos of cosmic origin are expected to be produced by hadronic interactions of cosmic rays in their acceleration sites, and can escape without absorption nor deflection to reach the Earth. The existence of an astrophysical neutrino flux has been established by the IceCube collaboration with a high level of significance [1], with arrival directions of the neutrinos being compatible with isotropy. Recently, the first evidence of an association of a neutrino and a cosmic source has been reported [2], opening new perspectives for the identification of the sources of neutrinos and cosmic rays.

The present analysis uses a likelihood stacking method, allowing the significance of a global excess of neutrino events in correlation with different catalogs of sources to be assessed. The stacking method is able to detect a small excess distributed among a population of sources, that could be missed by standard individual point source searches (cf. [3]).

## 2. Data set

The data sample used in the present analysis consist of 8754 track-like events detected by the ANTARES neutrino telescope between January 29,2007 and December 31,2017, for an overall livetime of 3125.4 days. The search for point like sources requiring a very good angular resolution, the selection procedure has been optimized to detect a point-like source with an energy spectrum $\propto E^{-2}$. The selected tracks have estimated neutrino energies between $\sim$ 100 GeV and $\sim$ 1 PeV, with a median angular resolution better than $0.4^\circ$ above 10 TeV. The detailled description of the selection criteria can be found in [4].

## 3. Description of the method

An extended maximum likelihood method is used to distinguish between a signal + background hypothesis $H_1$ from the null hypothesis $H_0$ where only background is present. Two different approaches are used, the *template stacking* and the *individual stacking*: in the individual stacking method, an independent fit is performed for each source in the catalog, and the final test statistic is the sum over all the individual test statistics. In the template method, only one global fit is performed, where the signal probability term contains the sum of the sources contributions.

The template method is used for astrophysical catalogs, where the spatial density of sources invalids the hypothesis of independent fits, and the stacking method is used for the high energy IceCube tracks. The log-likelihood for both hypotheses $H_0$ and $H_1$ is written as:

$$\ln \mathscr{L}(\mathrm{H}_1|x) = \sum_i^N \ln\left[\mu_s S(x_i) + \mu_b B(x_i)\right] - \mu_s - \mu_b \qquad \ln \mathscr{L}(\mathrm{H}_0|x) = \sum_i^N \ln\left[\mu_b B(x_i)\right] - \mu_b$$

where $N$ is the total number of observed neutrino candidates, $S(x_i)$ is the PDF of the signal and $B(x_i)$ the PDF of the background. The free parameters of the fit are the estimated number of signal events $\mu_s$ and background events $\mu_b$.

The test statistic is then defined as:

$$TS = \ln\left(\frac{\max(\mathscr{L}(\mathrm{H}_1|x))}{\max(\mathscr{L}(\mathrm{H}_0|x))}\right).$$

In the individual stacking method, the test-statistic takes the form:

$$TS = \frac{1}{\sum w} \sum_{j=1}^{N^{\mathrm{sources}}} w_j TS_j$$

where $TS_j$ is the local test statistic obtained for the $j^{\mathrm{th}}$ source, carrying a weight $w_j$.

Even if the global significance is evaluated via the total test statistic TS, the relative contribution of each source can be examined by looking at the distribution of individual test statistics $TS_j$.

In the template stacking method, only one fit is performed where the signal term is writen as:

$$S(x_i) = \frac{1}{\sum w} \sum_{j=1}^{N^{\mathrm{sources}}} w_j s_j(x_i)$$

where $s_j(x_i)$ is the pdf for the $j^{\mathrm{th}}$ single point source, with weight $w_j$.

The weight of the $j^{\mathrm{th}}$ source is defined as: $w_j = w_{\mathrm{model}} \times \mathscr{A}(\delta_j)$, where the $w_{\mathrm{model}}$ part is a quantity proportionnal to an emitted neutrino flux and $\mathscr{A}$ is the acceptance of the ANTARES tracks sample (assuming an $E^{-2}$ spectrum). The different assumptions on $w_{\mathrm{model}}$ are described in the following section.

As the relation between EM and neutrino flux is rather uncertain, the stacking analysis is also applied with an equal flux assumption, where $w_{\mathrm{model}} = 1$ for all sources in the likelihood. This provides a model-independent test, that could be more sensitive if the weights in the likelihood are very different from the true (unknown) ones.

## 4. Target sources

### 4.1 IceCube HE tracks

The sample consist of 56 events (55 in the FoV of ANTARES): 35 tracks from the IceCube 8 yr up-going muons with deposited energy above 200 TeV [5] and 21 additional tracks from the 6 yr HESE sample [6]. The majority of those events are located in the Northern hemisphere, with angular errors varying from $\sim 0.5°$ up to $\sim 5°$. A complementary study of the correlation between IceCube high energy tracks and ANTARES point source data is reported in these proceedings [3], where each track is considered separately.

### 4.2 Fermi 3LAC Blazars

The Fermi 3LAC catalog [7] contains 1420 blazars (clean sample) detected in gamma-rays between $1-100$ GeV by Fermi in 4 years of operation. The previous release (Fermi 2LAC) has been used by the IceCube collaboration in a stacking analysis [8], where several sub-classes of objects have been tested. A similar approach is followed here: in addition to the full Fermi 3LAC catalog, two additional sub-samples are also considered: the BL Lacs (604 objects), and the FSRQ sample (414 objects). The measured spectral slope of the gamma energy spectrum is taken into account in the weights, by computing the energy flux: $w_{\text{model}} = \int E \times \Phi_0 \left(\frac{E}{E_0}\right)^{-\gamma} dE$ where the integral runs over the Fermi energy range [1 GeV-100 GeV].

### 4.3 Star Forming Galaxies

A catalog of 64 Star Forming Galaxies (SFG) published by Fermi [9] was used recently by the Pierre Auger Collaboration, reporting a 3.9$\sigma$ correlation [10] with ultra high energy cosmic rays (UHECRs) with energy above 40 EeV. The SFG do not have an active nucleus, but have a strong star formation rate, with intense IR radiation fields that can act as target photons for the cosmic rays that are trapped in the strong galactic magnetic field. The following weights are used: $w_{\text{model}} = L_{\text{IR}}/d^2$ where $L_{\text{IR}}$ is the total IR luminosity ($8-1000\mu m$) and $d$ is the distance to the source.

### 4.4 Dust obscured AGN

The authors of [11] suggest to consider AGNs with high-energy jet pointing towards Earth, and going through a high quantity of dust, thus enhancing neutrino production via p-p interactions. The sample is built from cross-correlating objects from a radio-galaxy catalog [12] with the Fermi 2LAC catalog [13]. The selection process of the authors leads to a small catalog of 15 objects. To take into account the distance and the intrinsic luminosity, the X-ray flux is used as a weight: $w_{\text{model}} = \Phi_{\text{X}}$

### 4.5 Giant Radiogalaxies

Finally, a sample of 65 giant radiogalaxies sugested by L.Bassani et al. [14] is considered. The authors looked at extended radio galaxies in the sample of soft gamma ray (20-100keV) selected AGN in either the INTEGRAL or SWIFT-BAT surveys. The sample contains the brightest and most accretion-efficient radio galaxies in the local sky that have a clearly identified double lobed radio morphology. Among the published list of objects, one source without redshift information is removed, and Centaurus A is excluded because it cannot be considered as a point source (the angular extension of its radio lobes is $\sim 10°$). The weight $w_{\text{model}} = L_\gamma/d^2$ is used, where $L_\gamma$ is the luminosity measured in soft-gamma ray by SWIFT-BAT[1] and $d$ is the distance to the source.

## 5. Results

The results of the stacking analysis are summarized in table 1. The pre-trial p-values are labelled as $p$, and the post-trial as $P$. The trial factor computation has been performed by generating $10^4$ pseudo-experiments with pure background events, and applying the likelihood analysis for all combinations of catalogs and weighting schemes considered in this analysis. The most significant result is obtained for the radiogalaxy catalog for the equal weights hypothesis, with a pre-trial p-value equivalent to a 2.8$\,\sigma$ excess, reducing to 1.6$\,\sigma$ post-trial.

[1]except for 5 galaxies where the luminosity measured by INTEGRAL is used.

| | Equal weighting | | | | Flux weighting | | | |
|---|---|---|---|---|---|---|---|---|
| Catalog | TS | p | P | $\Phi^{UL}_{90\%}$ | TS | p | P | $\Phi^{UL}_{90\%}$ |
| Fermi 3LAC All Blazars | 6.15 | 0.19 | 0.83 | 4.1 | 0.21 | 0.85 | 1. | 2.0 |
| Fermi 3LAC FSRQ | 0.83 | 0.57 | 0.97 | 2.1 | $\sim 0$ | $\sim 1$ | 1. | 1.7 |
| Fermi 3LAC BL Lacs | 8.3 | 0.088 | 0.64 | 4.6 | 0.84 | 0.56 | 0.96 | 1.9 |
| Radio-galaxies | 3.4 | $4.8\ 10^{-3}$ | 0.10 | 3.3 | 5.1 | $6.9\ 10^{-3}$ | 0.13 | 3.7 |
| Star Forming Galaxies | 0.030 | 0.37 | 0.93 | 1.9 | $\sim 0$ | $\sim 1$ | 1. | 1.6 |
| Obscured AGN | $1.0\,10^{-3}$ | 0.73 | 0.98 | 1.4 | $\sim 0$ | $\sim 1$ | 1. | 1.3 |
| IC HE Tracks | 0.77 | 0.05 | 0.49 | 0.96 | - | - | - | - |

**Table 1:** Results of the likelihood stacking analysis. The 90% C.L flux upper limits are expressed in terms of equivalent diffuse $E^{-2}$ flux for the astrophysical catalogs (in units of $10^{-9}$ GeV$^{-1}$·cm$^{-2}$·s$^{-1}$·sr$^{-1}$). For the IceCube HE tracks, the upper limit is expressed in terms of flux per source $<\Phi_0>=\Phi_{\rm Tot}/N_{\rm sources}$, in units of $10^{-9}$ GeV$^{-1}$·cm$^{-2}$·s$^{-1}$ .

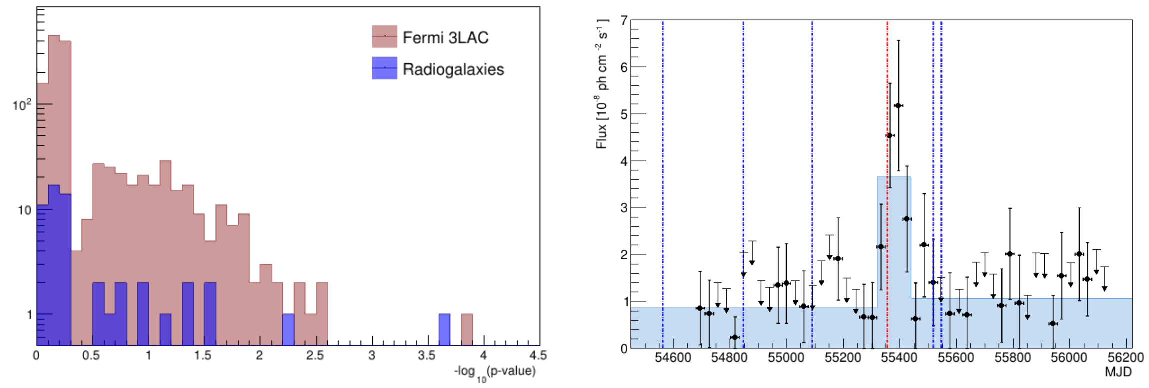


**Figure 1:** *Left*: Distribution of the individual p-values for the Fermi 3LAC blazars and for the radiogalaxies. *Right*: Fermi estimated gamma-ray flux for the BL Lac 3FGL J22551.1+2411, as a function of time (black points). The blue histogram represents the model gamma-ray light curve that is used in the time dependent likelihood (obtained via bayesian block algorithm). The blue vertical lines indicate the arrival time of ANTARES events located at an angular distance less than 2° from the blazar. The vertical red line corresponds to the arrival time of the IceCube track #3.

### 5.1 Search for dominant sources

To search for a possible dominant contribution of a small number of sources, the indvidual p-value associated to each source has been computed for the radiogalaxies and for the Fermi 3LAC blazars. The result is shown in figure 1 (left). For each catalog, a single source is present in the tail of the distribution of p-values, their properties are reported in the following section.

**Radiogalaxies** The radiogalaxy with the smallest p-value is 3C403, located at a distance of $\sim 260$ Mpc, that is found with a pre-trial p-value of $p = 2.3 10^{-4}$, equivalent to $3.7\sigma$. The probability to find by chance a similar excess among the $N = 56$ radiogalaxies in the field of view of ANTARES can be estimated as $P(n > 1) = 1 - P(0) = 1 - (1 - p)^N \simeq 1.3 10^{-2}$, equivalent to $2.5\sigma$. The arrival

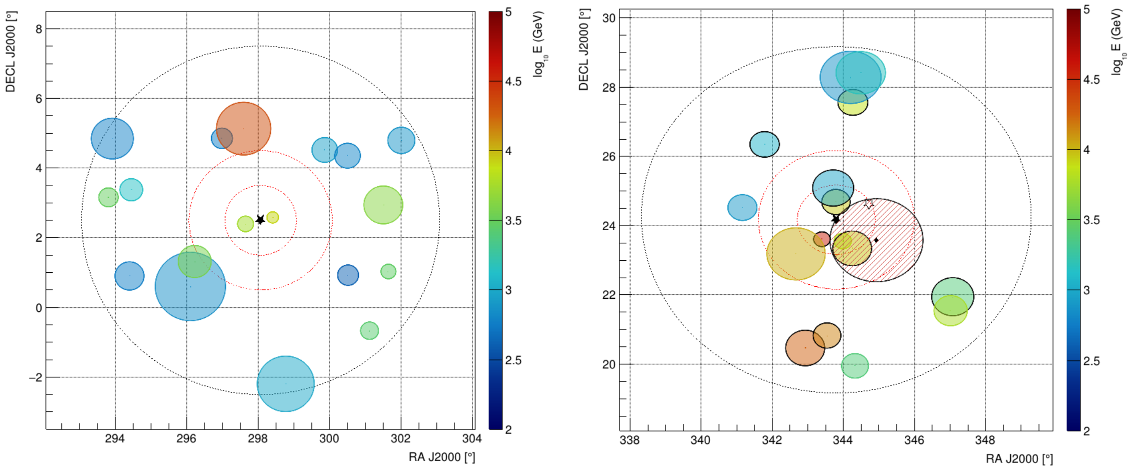


**Figure 2:** Arrival directions of ANTARES events in equatorial coordinates around the most prominent sources: *left*: radiogalaxy 3C403, *right*: blazar MG3 J225517+2409. Each event is represented by a filled circle with a radius equal to its angular error estimate. The estimated energy of the event is indicated by the color code. The concentric circles (dashed lines) centered around the source (black star marker) indicate the 1°, 2° (red) and 5° (black) angular distances to the source. On the right plot, the nearby Fermi source 3FGL J2258.8+2437 is indicated as a empty star marker, and the position of the IceCube track by the red-hashed circle with a black diamond marker. The ANTARES events that do have arrival times within the range of the available Fermi blazar light curve are circled by a bold black line.

direction of ANTARES events around this source are shown in figure 2 (left), where one can see that the excess comes from the presence of 2 events lying at less than 0.5° of the source. Those track events have an estimated angular uncertainty of 0.2°, and a reconstructed energy of $\sim 5$ and $\sim 10$ TeV.

**Blazars** The most significant blazar from the Fermi 3LAC catalog is MG3 J225517+2409 (corresponding to Fermi 3FG J2255.1+2411), classified as BL Lac and LSP (Low Synchrotron Peak) and with unknown redshift. The associated pre-trial p-value is $1.4 \times 10^{-4}$, equivalent to $3.8\sigma$. The probability to find by chance a similar excess among the $N = 1255$ blazars in the field of view of ANTARES is estimated as $P(n > 1) = 1 - (1-p)^N \simeq 0.16$, equivalent to $1.4\sigma$. The distribution of ANTARES events around the blazar is shown in figure 2 (right).

There are 5 ANTARES tracks lying at less than 1° from the source, with estimated energies ranging from $\sim 3$ to $\sim 40$ TeV, and with estimated angular uncertainty between 0.2° and 0.5°. In addition, a high energy muon track (ID=3) from the IceCube 8 yr up-going muons sample [5] is found to lie at an angular distance of 1.1° from the source. The association between these ANTARES events and this particular IceCube high energy track has been studied by an independent analysis [3], finding a $2.4\sigma$ trial-corrected significance.

### 5.2 Dedicated analysis of region around the blazar MG3 J225517+2409

The possible association between ANTARES and IceCube neutrinos and the blazar MG3

J225517+2409 is investigated in more detail, by looking at the time evolution of the gamma-ray emission of the source. The Fermi 3FGL light curve [15] available online for this source is shown in figure 1 (right), together with the arrival times of ANTARES and IceCube events. The time evolution of the gamma-ray flux above 100 MeV is shown in 48 bins of 30 days, from August 2008 to July 2012. The flux increases by a factor $\sim 5$ in a time window of $\sim 4$ months, centered around $MJD = 55400$ (July 2010). Two ANTARES events occur 4 and 5 months after this maximum, and the IceCube track # 3 is detected within the flaring period.

It is noteworthy that a candidate blazar 3FGL J2258.8+2437 is located only $\sim 1^\circ$ away from MG3 J225517+2409. This additional source does not have an identified counterpart, and therefore is not present in the Fermi 3LAC sample that is studied. For the present analysis, this source is not considered in the chance coincidence calculation.

**Time analysis** The results of a preliminary estimation of the significance of both space and time correlation between the neutrinos detected by ANTARES and the blazar MG3 J225517+2409 with a time dependent likelihood are reported. The strength of such a correlation for the 56 IceCube high energy neutrinos is evaluated, and provide an order of magnitude of the combined p-value that can be expected.

The likelihood expression is modified:

$$\ln \mathscr{L}(\mathrm{H}_1|x) = \sum_i^N \ln\left[\mu_s S(x_i) f_S(t_i) + \mu_b B(x_i) f_B(t_i)\right] - \mu_s - \mu_b$$

where $f_S(t_i)$ and $f_B(t_i)$ represent the signal and background time PDFs respectively. A bayesian block algorithm [16] is applied to obtain the model light curve of MG3 J225517+2409 (figure 1) that is used as the signal time PDF. The distribution of real ANTARES events with relaxed quality cuts is used to compute the background time PDF.

The result of likelihood fit applied on all ANTARES 11 yr data gives a pre-trial p-value of $p = 1.4 \times 10^{-4}$, equivalent to $3.7\sigma$. Since the ANTARES events do not fall during the flaring period, this p-value is equal to the time integrated one $p = 1.4 \times 10^{-4}$ that is reported in the previous section.

A time dependent likelihood analysis is also performed for the IceCube high energy tracks, where the spatial PSF is taken as a two dimension gaussian function with $\sigma = 1.5 \times \beta$ where $\beta$ is the 50% C.L statistical angular errors reported in [5]. The background distribution $A(\sin\delta)$ is estimated from the real distribution of the IceCube tracks declinations, and the time distribution of events is assumed to be constant. The p-value obtained for the 56 IceCube tracks is $p = 1.6 \times 10^{-3}$, equivalent to $3.2\sigma$.

An order of magnitude of the combined ANTARES-IceCube p-value can then be estimated to be $p_{\mathrm{Combined}} = p_{\mathrm{ANT}} \times p_{\mathrm{IC}} \sim 2.2 \times 10^{-7}$, equivalent to $\sim 5.2\sigma$ pre-trial. However, this result relies on the assumption that the neutrino flux is produced continuously by the source. Under this hypothesis, the neutrino flux (for $E^{-2}$ spectrum) of MG3 J225517+2409 is estimated to be $\sim 1 - 3 \times 10^{-8}$ GeV$^{-1}$·cm$^{-2}$·s$^{-1}$·sr$^{-1}$, depending on the number of neutrinos candidates that are considered as signal (between 2 and 5).

In contrast, one could assume that the neutrino production occurs only during the flaring activity of the considered blazar. The likelihood analysis is then repeated with a time PDF equal to zero outside the flare period (4 bins around $MJD = 55400$): the p-value for ANTARES is $\sim 1$ because no signal events are found, and $p = 5 \times 10^{-4}$ for the IceCube events. The combined p-value in this case would then be $p_{\text{Combined}} \sim 5 \times 10^{-4}$, equivalent to $3.5\sigma$.

## 6. Conclusion

The results of a stacking point source likelihood search using 11 years of ANTARES data have been presented. After accounting for trial factors, none of the catalog considered have shown a significant result in the stacking analysis. The most significant value is obtained for the radiogalaxy catalog, with a pre-trial value of $4.8 \times 10^{-3}$, reducing to 0.1 post-trial. However, individual sources such as the radiogalaxy 3C403 and the blazar MG3 J225517+2409 are reported as interesting targets. In addition, a dedicated time analysis has been performed in the case of MG3 J225517+2409, providing a preliminary estimation of $\sim 2.2 \times 10^{-7}$ pre-trial for the chance coincidence of observing such an association between ANTARES and IceCube neutrinos in space and time correlation with the blazar. This p-value is higher, $p \sim 5. \times 10^{-4}$, if one assumes that the neutrino emission occurs only during the blazar's flaring period.

**Acknowledgments** The authors thank Loredana Bassani and Sara Buson for fruitful discussions on the radiogalaxy catalog, and on the Fermi data analysis, respectively.

## References

[1] IceCube Collaboration. *Phys. Rev. Lett.*, 113:101101, Sep 2014.

[2] IceCube collaboration. *Science*, 361(6398):147–151, 2018.

[3] G. Illuminati et al. (ANTARES collaboration). *PoS(ICRC2019)1177*.

[4] A. Albert et al. (ANTARES Collaboration). *Phys. Rev. D*, 96:082001, 2017.

[5] C. Haack and C. Wiebusch et al. (IceCube collaboration). *ICRC 2017, PoS:1005*, 2017.

[6] M. G. et al. (IceCube Collaboration). *(ICRC 2017), PoS:981*, 2017.

[7] M. Ackermann and M. Ajello et al (Fermi collaboration). *ApJ*, 810:14, 2015.

[8] IceCube Collaboration. *The Astrophysical Journal*, 835:45, 2017.

[9] A. Abdo, M. Ackermann, and M. Ajello et al. (Fermi collaboration). *The Astrophysical Journal*, 755:164, 2012.

[10] A.Aab et al. (The Pierre Auger Collaboration). *The Astrophysical Journal*, 853(2):L29, 2018.

[11] G. Maggi et al. Physical Review D 94, 103007 (2016).

[12] P. Schellart N. Nierstenhöfer S. van Velzen, H. Falcke and K.H. Kampert. A&A 544, A18 (2012).

[13] M. Ajello et al. (Fermi collaboration) M. Ackermann. *The Astrophysical Journal*, 743(2):171, 2011.

[14] L.Bassani et al. *MNRAS*, 461:3165–3171, 2016.

[15] F. Acero, M. Ackermann, M. Ajello, A. Albert, W. B. Atwood, M. Axelsson, L. Baldini, J. Ballet, G. Barbiellini, and D. Bastieri. *ApJS*, 218(2):23, 2015.

[16] B. Jackson, J.D Scargle, J.P. Norris, and J. Chiang. *Astrophys. J*, 764(167), 2013.